Available online at www.sciencedirect.com
SCIENCE DIRECT®
Journal of Solid State Chemistry 177 (2004) 2714–2725
JOURNAL OF SOLID STATE CHEMISTRY
http://elsevier.com/locate/jssc

$Cu_2Sc_2Ge_4O_{13}$, a novel germanate isotypic with the quasi-1D compound $Cu_2Fe_2Ge_4O_{13}$ between 100 and 298 K

G.J. Redhammer[a,b,*] and G. Roth[a]

[a] *Institute of Crystallography, Technical University (RWTH)-Aachen, Jägerstrasse 17/19, Aachen D-52056, Germany*
[b] *Institute of Mineralogy, University of Salzburg, Hellbrunnerstr. 34, Salzburg A-5020, Austria*

Received 1 December 2003; received in revised form 27 March 2004; accepted 2 April 2004

Abstract

The germanate compound $Cu_2Sc_2Ge_4O_{13}$ has been synthesized by solid-state ceramic sintering techniques between 1173 and 1423 K. The structure was solved from single-crystal data by Patterson methods. The title compound is monoclinic, $a = 12.336(2)$ Å, $b = 8.7034(9)$ Å, $c = 4.8883(8)$ Å, $\beta = 95.74(2)$, space group $P2_1/m$, $Z = 4$. The compound is isotypic with $Cu_2Fe_2Ge_4O_{13}$, described very recently. The structure consists of crankshaft-like chains of edge-sharing ScO_6 octahedra running parallel to the crystallographic *b*-axis. These chains are linked laterally by $[Cu_2O_6]^{8-}$ dimers forming a sheet of metal–oxygen–polyhedra within the *a*–*b* plane. These sheets are separated along the *c*-axis by $[Ge_4O_{13}]^{10-}$ units. Cooling to 100 K does not alter the crystallographic symmetry of $Cu_2Sc_2Ge_4O_{13}$. While the *b*, *c* lattice parameter and the unit cell volume show a positive linear thermal expansion ($\alpha = 6.4(2) \times 10^{-6}$, $5.0(2) \times 10^{-6}$ and $8.3(2) \times 10^{-6}\,K^{-1}$ respectively), the *a* lattice parameter exhibits a negative thermal expansion ($\alpha = -3.0(2) \times 10^{-6}\,K^{-1}$) for the complete *T*-range investigated. This negative thermal expansion of *a* is mainly due to the increase of the Cu–Cu interatomic distance, which is along the *a*-axis. Average bond lengths remain almost constant between 100 and 298 K, whereas individual ones partly show both significant shortages and lengthening.

Keywords: Germanate compound; Structure determination; Low temperature; Chain structure

1. Introduction

Very recently, a new structure type, $Cu_2Fe_2Ge_4O_{13}$ was discovered by Redhammer and Roth [1] and independently described a few months later by Masuda et al. [2]. The structure is monoclinic and contains crankshaft-like chains of edge-sharing Fe^{3+} octahedra which are cross-linked laterally by square-planar coordinated Cu^{2+} ions. These metal–ion–oxygen sheets are separated by a chain of four corner-sharing GeO_4 tetrahedra. The structure of $Cu_2Fe_2Ge_4O_{13}$ has a distinct low-dimensional character and fits well into the group of low-dimensional spin materials, such as $CuGeO_3$ [3,4]. The compound represents a mixed-spin system, which poses new challenges to the investigation of quantum spin systems in solid-state science due to their higher complexity. First investigations on $Cu_2Fe_2Ge_4O_{13}$ exhibit that magnetic ordering in $Cu_2Fe_2Ge_4O_{13}$ indeed is complex. Magnetic susceptibility and specific heat measurements show two events taking place at 100 and 40 K [1,5]. The latter one corresponds to the 3D magnetic ordering of the compound [5], the first one to ordering phenomena within the Cu^{2+}-sublattice.

In the present contribution we report the synthesis and crystal structure determination of $Cu_2Sc_2Ge_4O_{13}$ a compound analogous to $Cu_2Fe_2Ge_4O_{13}$, in which the paramagnetic Fe^{3+} is completely substituted by the diamagnetic Sc^{3+}. Besides crystal chemical and structure topological aspects the results of this study will allow studying the magnetic properties of a simple-spin system which helps to interpret the results obtained for the mixed-spin system $Cu_2Fe_2Ge_4O_{13}$.

*Corresponding author. Institute of Mineralogy, University of Salzburg, Neuhofen 224/TOP 1, A-4910 Ried im Innkreis, Austria. Fax: +43-662-8044-622.
E-mail address: guenther.redhammer@aon.at (G.J. Redhammer).

0022-4596/$ - see front matter © 2004 Elsevier Inc. All rights reserved.
doi:10.1016/j.jssc.2004.04.016

2. Experimental

2.1. Synthesis

A mixture of CuO, Sc_2O_3 and GeO_4, weighted in the correct proportions of $Cu_2Sc_2Ge_4O_{13}$, was carefully ground under alcohol, pressed into pellets, put into an open platinum crucible and fired under ambient pressure and ambient oxygen fugacity at 1173 K in a temperature range between 1173 and 1373 K. After each of six heating cycle, the sample material was reground, pressed and reheated. The product consisted of a mixture of the title compound and $CuGeO_3$. The amount of $CuGeO_3$ decreased successively as synthesis temperature and heating time were increased. In a final synthesis cycle, the sample was fired at 1423 K and a coarse grained single phase product of $Cu_2Sc_2Ge_4O_{13}$ was obtained, from which single crystals could be selected. The total synthesis time was 69 days. $Cu_2Sc_2Ge_4O_{13}$ melts incongruently between 1423 and 1448 K.

2.2. Single-crystal X-ray diffraction

A pale green cuboid crystal of $Cu_2Sc_2Ge_4O_{13}$ ($0.11 \times 0.10 \times 0.08\,mm^3$ in size, formula weight $M = 715.36$ g/mol, absorption coefficient $\mu = 16.630$ mm^{-1} for Mo$K\alpha$) was used for single-crystal X-ray diffraction experiments. Intensity data sets were collected on a Stoe IPDS II imaging-plate diffractometer system (Mo$K\alpha$ radiation, pyrolytic graphite monochromator), equipped with a cryo-stream liquid N_2-cryostat (85…300 K, accuracy at least 1 K). Intensity data were collected up to 65.0° in 2θ within an ω-range of 0–180° and two different φ positions in most cases; the ω rotation during exposure was 1.5° per frame, the crystal to detector distance 80 mm and the exposure time 3 min. Data sets were collected at 100, 150, 200, 250, and 290 K. Absorption correction was done empirically via symmetry equivalents using the SHAPE-software [6]. Structure solution (using Patterson methods) and subsequent refinement was carried out with the programs SHELXS-97 and SHELXL-97 [7] as implemented in the program suite WinGX 1.64.05 [8]. X-ray scattering factors in their ionic form, together with anomalous dispersion coefficients were taken from the International Tables for Crystallography [9]. Structural drawings were made with DIAMONDS 2.0B [10]. Bond valence calculations were made with the program VaList [11] using bond valence parameters of [12]. To test for hysteresis effects, the title compound was re-measured at 298 K after cooling to 100 K. The results are identical to those of the measurement at 298 K before cooling within experimental error.

In most of the figures, regression lines where fitted to the data to clarify trends. These regressions correspond to polynomials of 1st (linear) or 2nd (quadratic) order: $y = a_0 + a_1 \times x + a_2 \times x^2$. Second order polynomial functions were used, when distinct curvatures where visible by eye in the data courses. Regression fit values were above 0.9 in almost all fits. These fits are purely mathematically in nature and should serve as guides to the eye, they have no physical meaning.

3. Results and discussion

The analysis of systematic absences indicated the space group $P2_1/m$ for $Cu_2Sc_2Ge_4O_{13}$, which is the same as the one for $Cu_2Fe_2Ge_4O_{13}$ [1,2]. Structure solution on the 298 K data yielded a model which was very similar to the one obtained for the Fe-analogue. Full-matrix least-squares refinements based on F^2 using anisotropic displacement parameters converged to final agreement factors of $R_1 < 4.0\%$ for all data sets. Table 1 contains a summary of experimental conditions during data collection and the structural refinement parameters; Table 2 gives the refined atomic coordinates and equivalent isotropic displacements parameters (the anisotropic displacement parameters are given in the Crystallographic Information File, CIF) and Table 3 compiles selected bond lengths, bond angles and distortion parameters.

Compared to $Cu_2Fe_2Ge_4O_{13}$ [1] ($a = 12.103(2)$ Å, $b = 8.5159(9)$ Å, $c = 4.8792(8)$ Å, $\beta = 96.19(2)$ Å), the lattice parameters in the Sc analogue are larger by about 0.2 Å for the a and b direction, the c lattice parameter is nearly identical in both compounds and the monoclinic angle is $\approx 0.45°$ smaller in $Cu_2Sc_2Ge_4O_{13}$ as compared to $Cu_2Fe_2Ge_4O_{13}$. Bond valence calculations for the 298 K structure yield a bond valence sum of 3.98 valence

Table 1
Lattice parameters of $Sc_2Cu_2Ge_4O_{13}$ between 100 and 300 K

T (K)	a (Å)	b (Å)	c (Å)	β (deg)	V (Å^3)
100	12.3437(19)	8.6925(9)	4.8831(8)	95.713(21)	521.34(9)
150	12.3414(20)	8.6939(9)	4.8841(8)	95.719(13)	521.43(8)
200	12.3397(20)	8.6976(9)	4.8856(8)	95.727(13)	521.73(9)
250	12.3379(20)	8.6997(9)	4.8863(8)	95.732(13)	521.85(9)
298	12.3361(20)	8.7034(9)	4.8883(8)	95.738(13)	522.21(8)
300[a]	12.33614(16)	8.7032(6)	4.8877(5)	95.737(9)	522.13(6)

[a] 300 K data are determined from Si-calibrated powder X-ray diffraction data using full pattern refinement (Le-Bail method).

Table 2
Data collection parameters and results of structure refinement for $Cu_2Sc_2Ge_4O_{13}$ at different temperatures

	100 K	150 K	200	250 K	298 K
Space group	$P2_1/m$	$P2_1/m$	$P2_1/m$	$P2_1/m$	$P2_1/m$
Z	2	2	2	2	2
Density$_{(calc)}$ (mg/m^3)	4.557	4.556	4.554	4.553	4.549
θ range data collection (deg)	2.9–32.1	2.9–32a.1	2.9–32.1	2.9–32.1	2.9–32.1
Index range					
h	−18…18	−18…18	−18…18	−18…18	−18…18
k	−12…10	−12…10	−12…10	−12…10	−12…10
l	−7…7	−7…7	−7…7	−7…7	−7…7
Reflections collected	6161	6166	6168	6185	6190
Independent refl.	1893	1896	1896	1899	1900
Transmission (min)	0.104	0.105	0.101	0.103	0.106
Transmission (max)	0.182	0.179	0.180	0.174	0.176
R_{int} (%)	7.47	6.58	6.74	6.69	7.09
Completeness of data (%)	98.1	98.3	97.9	98.1	98.0
Number of parameters	110	110	110	110	110
R_1 index [$I>2\sigma$] (%)	3.93	3.90	3.91	4.04	3.77
R_1 all data (%)	6.37	6.14	6.45	6.69	6.92
wR_2 index [$I>2\sigma$] (%)	6.64	6.11	6.13	6.33	6.49
wR_2 all data (%)	7.14	6.60	6.66	6.84	7.26
Goodness-of-fit on F^2	1.097	1.084	1.079	1.071	1.049
Extinction coefficient	0.0051(5)	0.0064(4)	0.0075(5)	0.0077(4)	0.0083(5)
Largest diff. Peak (e Å^{-3})	1.072	1.302	1.432	1.558	1.129
Largest diff. hole (e Å^{-3})	−1.098	−1.405	−1.5387	−1.116	−1.177

units (vu) for the Ge(1) site, the Ge(2)–Ge(4) sites are slightly oversaturated (4.09, 4.05 and 4.05 vu, respectively). Sc reveals a bond valence sum of 2.96 vu; for Cu^{2+} a valence sum of 1.88 vu was obtained. The situation does not change significantly towards low temperature. The obtained valence sums are in perfect agreement with the valences of the cations with the exception of Cu^{2+} which is known to deviate substantially from the expected value of 2.0.

3.1. Topology of the structure at 298 K

The main building units of the structure are infinite chains of Sc^{3+} octahedra, running parallel the b-axis. These chains are interconnected along the a-axis by Cu-dimers, forming a slightly buckled cation-sheet of Cu and Sc sites within the a–b plane (Fig. 1). These sheets are separated along the c-axis by small chains (tetramers) of four corner-sharing and symmetrically distinct GeO_4 tetrahedra. These Ge_4O_{13} units are aligned parallel to the crystallographic a-axis and perpendicular to b and are slightly bent, as can be seen in the projection onto the a–c plane. They are not connected to each other (Fig. 1).

Sc^{3+} is in 6-fold oxygen coordination. These Sc^{3+}-octahedra share two common edges with neighboring Sc^{3+} octahedra, forming an infinite crankshaft like chain running parallel to the crystallographic b-axis. If one defines the O(6)–Sc^{3+}–O(4) direction as the apex–cation–apex axis of the octahedron, the individual octahedra show a *cis–trans* connection (Fig. 2). The O(6)–Sc^{3+}–O(4) bond angle [168.68(9)°] is the largest one within the octahedron. The Sc^{3+}–O bond lengths range between 2.057(3) and 2.162(4) Å (average value 2.112(4) Å). The mean Sc^{3+}–O bond length is longer than the mean Fe^{3+}–O bond length (2.036(2) Å, [1]) by 0.076 Å, which is very close to the difference in ionic radii between Fe^{3+} (0.645 Å) and Sc^{3+} (0.73 Å, [13]). The bond length distortion, BLD, amounts to 1.35(5)% (BLD = deviation of individual bond lengths from their mean value, [14]). This is a value indicative for quite low bond length deviation. In contrast to the rather uniform Sc–O bond lengths, the O–O edge lengths for the $Sc^{3+}O_6$ octahedron are quite diverse. O–O edges, shared with other topological building units (= e_s for "shared edges") are generally smaller than those, which are not shared (= e_u, unshared edges). The average shared edge takes a value of $e_s = 2.575(4)$ Å, the average unshared edge is $e_u = 3.113(3)$ Å. These unshared edges vary between 2.678(3) Å (O(1)–O(6) edge) and 3.533(3) Å (O(4)–O(6) edge). The ratio e_u/e_s is a measure of polyhedral distortion [15]. For quite regular octahedra, e_u/e_s ranges between 1.03 and 1.08 in Na–Li clinopyroxenes [16], between 1.08 and 1.12 in tri-octahedral micas [17]. For $Cu_2Sc_2Ge_4O_{13}$ e_u/e_s for the ScO_6 octahedron amounts to a value of as much as 1.20. Furthermore, the edge length distortion ELD [14], which measures the sum of the deviations of the individual edge lengths from their mean value, takes a high value of 9.60(5)%. All these findings point to a large polyhedral distortion of the Sc^{3+} site. The very large octahedral angle variance [14] with

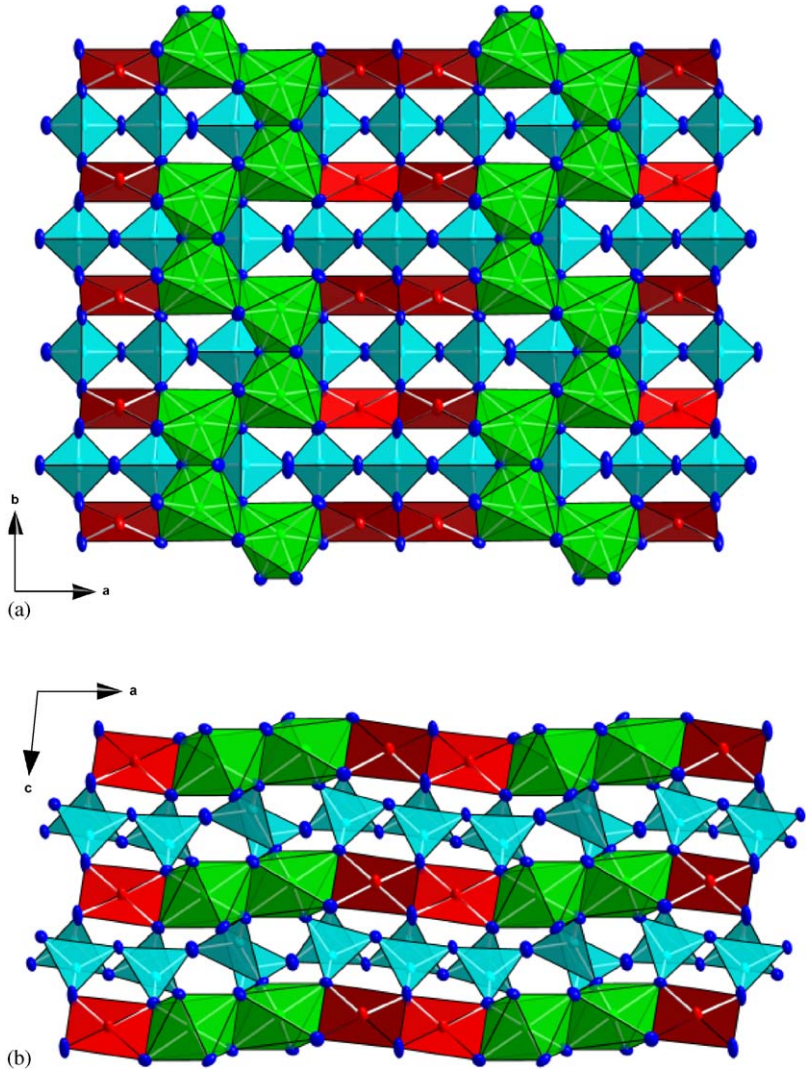

Fig. 1. Polyhedral representation of the $Cu_2Sc_2Ge_4O_{13}$ structure viewed normal to (001) (a) and normal to (010).

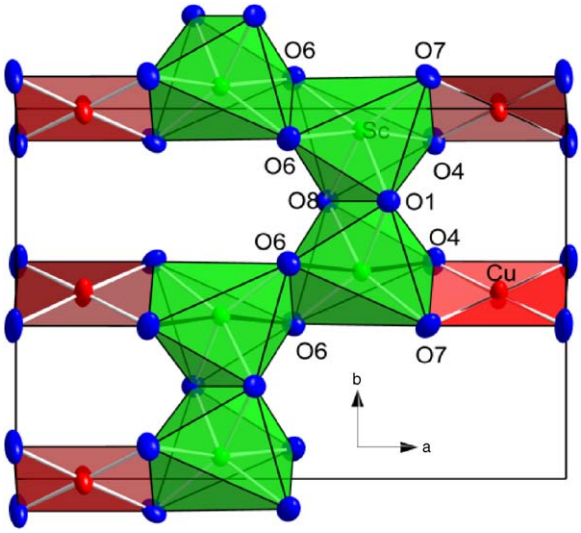

Fig. 2. Polyhedral representation of a detail of the $Cu_2Sc_2Ge_4O_{13}$ structure in a view normal to (001); GeO_4 tetrahedra are not shown, the longest axis of the octahedron O(6)–Sc–O(4) is high lightened.

OAV = 208.9(2)° also supports this argument. Within the $Sc^{3+}O_6$ chain, two different Sc–Sc interatomic distances can be identified. The shorter one is the one pointing in the *b*-direction [3.306(2) Å], the longer on [3.400(2) Å] points towards the *a*-direction.

Cu^{2+} is in a 4-fold planar coordination (Fig. 2). The Cu–O bond lengths range between 1.931(4) and 2.011(4) Å, the mean value being 1.961(4) Å. These Cu–O bond lengths are very similar to those in the isotypic compound $Cu_2Fe_2Ge_4O_{13}$ (mean Cu–O bond length = 1.964(4), [1]). The next nearest oxygen atoms are 2.860(4) and 2.957(4) Å away from the Cu^{2+} atom, thus they are assumed to be non-bonding oxygen atoms and a description as a 4-fold coordination of Cu seems to be appropriate: Two such CuO_4 planes are connected to each other via the common O(9)–O(9) edge, forming a Cu–Cu dimer. With 2.456(4) Å this shared edge is the shortest O–O edge of the CuO_4 plane. The Cu–Cu interatomic distance, which is parallel to the crystallographic *a* direction, amounts to 3.011(1) Å, which is

Table 3
Atomic positional parameters and equivalent isotropic displacement parameters for $Cu_2Sc_2Ge_4O_{13}$ at different temperatures

	x	y	z	U_{eq} (Å^2)
100 K				
Ge(1)	0.2317(1)	$\frac{1}{4}$	0.4967(1)	0.0044(1)
Ge(2)	0.7529(1)	$\frac{1}{4}$	0.3344(1)	0.0047(1)
Ge(3)	−0.0070(1)	$\frac{1}{4}$	0.3990(1)	0.0050(1)
Ge(4)	0.5143(1)	$\frac{1}{4}$	0.5998(1)	0.0044(1)
Sc(1)	0.3723(1)	0.0601(1)	1.0474(2)	0.0048(1)
Cu(1)	0.1229(1)	−0.0035(1)	1.0475(1)	0.0064(1)
O(1)	0.3226(4)	$\frac{1}{4}$	0.7930(10)	0.0053(8)
O(2)	0.6517(4)	$\frac{1}{4}$	0.5526(11)	0.0108(9)
O(3)	0.1061(1)	$\frac{1}{4}$	0.6435(5)	0.0087(9)
O(4)	0.2403(3)	0.0875(4)	0.2900(7)	0.0066(6)
O(5)	0.8730(4)	$\frac{1}{4}$	0.5645(10)	0.0071(8)
O(6)	0.5035(3)	0.0812(4)	0.7879(7)	0.0066(6)
O(7)	0.7502(3)	0.855(4)	0.1293(7)	0.0071(6)
O(8)	0.4332(4)	$\frac{1}{4}$	0.2868(10)	0.0058(8)
O(9)	−0.0039(2)	0.0861(4)	0.1976(7)	0.0091(7)
150 K				
Ge(1)	0.2316(1)	$\frac{1}{4}$	0.4964(1)	0.0050(1)
Ge(2)	0.7528(1)	$\frac{1}{4}$	0.3341(1)	0.0051(1)
Ge(3)	−0.0070(1)	$\frac{1}{4}$	0.3992(1)	0.0058(1)
Ge(4)	0.5143(1)	$\frac{1}{4}$	0.6000(1)	0.0050(1)
Sc(1)	0.3723(1)	0.0601(1)	1.0475(2)	0.0055(1)
Cu(1)	0.1228(1)	−0.0034(1)	1.0476(1)	0.0075(1)
O(1)	0.3227(3)	$\frac{1}{4}$	0.7930(5)	0.0072(8)
O(2)	0.6519(3)	$\frac{1}{4}$	0.5509(8)	0.0116(9)
O(3)	0.1060(4)	$\frac{1}{4}$	0.6433(10)	0.0082(8)
O(4)	0.2403(1)	0.0872(3)	0.2902(4)	0.0069(6)
O(5)	0.8729(2)	$\frac{1}{4}$	0.5647(8)	0.0079(8)
O(6)	0.5037(3)	0.0817(3)	0.7898(7)	0.0075(6)
O(7)	0.7496(2)	0.0856(3)	0.1300(7)	0.0086(6)
O(8)	0.4331(4)	$\frac{1}{4}$	0.2871(10)	0.0069(8)
O(9)	−0.0040(3)	0.0859(4)	0.1986(8)	0.0109(7)
200 K				
Ge(1)	0.2318(1)	$\frac{1}{4}$	0.4962(1)	0.0053(1)
Ge(2)	0.7527(1)	$\frac{1}{4}$	0.3336(1)	0.0057(1)
Ge(3)	−0.0071(1)	$\frac{1}{4}$	0.3992(2)	0.0063(1)
Ge(4)	0.5144(1)	$\frac{1}{4}$	0.5998(1)	0.0049(1)
Sc(1)	0.3722(1)	0.0601(1)	1.0472(2)	0.0053(1)
Cu(1)	0.1226(1)	−0.0032(1)	1.0474(1)	0.0085(1)
O(1)	0.3222(4)	$\frac{1}{4}$	0.7926(10)	0.0064(8)
O(2)	0.6523(4)	$\frac{1}{4}$	0.5505(11)	0.0134(9)
O(3)	0.1062(4)	$\frac{1}{4}$	0.6432(10)	0.0081(8)
O(4)	0.2402(3)	0.0875(4)	0.2902(7)	0.0074(6)
O(5)	0.8729(4)	$\frac{1}{4}$	0.5656(10)	0.0082(8)
O(6)	0.5038(2)	0.0814(3)	0.7905(7)	0.0073(6)
O(7)	0.7498(1)	0.0853(3)	0.1296(6)	0.0086(6)
O(8)	0.4330(3)	$\frac{1}{4}$	0.2866(6)	0.0076(8)
O(9)	−0.0042(3)	0.0862(4)	0.1979(8)	0.0112(7)
250 K				
Ge(1)	0.2318(1)	$\frac{1}{4}$	0.4961(1)	0.0060(1)
Ge(2)	0.7526(1)	$\frac{1}{4}$	0.3336(1)	0.0063(1)
Ge(3)	−0.0071(1)	$\frac{1}{4}$	0.3987(2)	0.0070(1)
Ge(4)	0.5143(1)	$\frac{1}{4}$	0.6000(2)	0.0055(1)
Sc(1)	0.3721(1)	0.0601(1)	1.0473(2)	0.0060(2)
Cu(1)	0.1225(1)	−0.0032(1)	1.0474(1)	0.0098(1)
O(1)	0.3227(3)	$\frac{1}{4}$	0.7915(6)	0.0072(8)
O(2)	0.6525(3)	$\frac{1}{4}$	0.5508(9)	0.0154(10)
O(3)	0.1061(3)	$\frac{1}{4}$	0.6429(8)	0.0091(9)
O(4)	0.2399(1)	0.0871(4)	0.2905(4)	0.0092(6)
O(5)	0.8724(4)	$\frac{1}{4}$	0.5640(10)	0.0096(9)
O(6)	0.5041(2)	0.0813(3)	0.7896(6)	0.0084(6)
O(7)	0.7493(3)	0.0854(4)	0.1297(7)	0.0097(9)
O(8)	0.4333(3)	$\frac{1}{4}$	0.2865(6)	0.0089(9)
O(9)	−0.0043(2)	0.0861(4)	0.1974(7)	0.0137(7)
298 K				
Ge(1)	0.2318(1)	$\frac{1}{4}$	0.4960(2)	0.0067(1)
Ge(2)	0.7526(1)	$\frac{1}{4}$	0.3333(2)	0.0071(1)
Ge(3)	−0.0071(1)	$\frac{1}{4}$	0.3987(2)	0.0087(2)
Ge(4)	0.5143(1)	$\frac{1}{4}$	0.5999(2)	0.0062(1)
Sc(1)	0.3721(1)	0.0601(1)	1.0472(2)	0.0067(2)
Cu(1)	0.1225(1)	−0.0035(1)	1.0475(1)	0.0113(1)
O(1)	0.3226(4)	$\frac{1}{4}$	0.7904(10)	0.0081(1)
O(2)	0.6517(4)	$\frac{1}{4}$	0.5482(13)	0.0197(12)
O(3)	0.1061(4)	$\frac{1}{4}$	0.6427(11)	0.0108(9)
O(4)	0.2403(3)	0.0870(4)	0.2897(7)	0.0102(7)
O(5)	0.8723(4)	$\frac{1}{4}$	0.5644(11)	0.0114(9)
O(6)	0.5042(3)	0.0812(4)	0.7904(7)	0.0098(6)
O(7)	0.7491(2)	0.0858(4)	0.1291(7)	0.0105(7)
O(8)	0.4335(4)	$\frac{1}{4}$	0.2884(11)	0.0094(9)
O(9)	−0.0043(3)	0.0866(5)	0.1970(9)	0.0152(8)

slightly smaller than in $Cu_2Fe_2Ge_4O_{13}$ (3.025(1) Å, [1]), even though the a unit cell parameter is larger in the title compound. The Cu–O9–Cu bond angle is 101.63(8)°. The Cu-dimer shares two of its edges (O(4)–O(7) edge, Fig. 2) with two different crankshaft-like ScO_6-octahedral-chains, and thus bridges them in the a direction. This shared edge (2.554(4) Å) again is distinctly shorter than the unshared edges O(4)–O(9) and O(7)–O(9) (3.006(4) and 3.028(4) Å, respectively). As can be seen in Figs. 3 and 4, the Cu-dimers are inclined with respect to the a-axis and the inclination angle alternates along the $+b$ and in $-b$ direction.

The metal cation layers are separated from each other along the crystallographic c-axis by layers of GeO_4 tetrahedra. There are four symmetrically distinct GeO_4 tetrahedra, which are connected to each other via a common corner forming a Ge_4O_{13} chain, which is slightly bent (Fig. 3a). The bridging angle O(1)–O(3)–O(5) amounts to 172.2(1)°, the O(3)–O(5)–O(2) bridging angle 174.1(1)° and the O(5)–O(2)–O(6) angle is as low as 134.7(1)° only (Fig. 4). The Ge(1)–Ge(3) tetrahedra show the same orientation, whereas the $Ge(4)O_4$ tetrahedron is turned around 180°. The turn around of the Ge(4) site is necessary as only by this rotation by 180° it is possible to fit $Ge(4)O_4$ tetrahedron into the cavity which is formed by the two ScO_6 chains below and above the tetrahedral layer. The $Ge(1)O_4$ tetrahedron is the largest of the four. Its Ge–O bond lengths range between 1.734(3) and 1.773(3) Å, the mean value is 1.751(3) Å, the polyhedral volume amounts to 2.73(1) Å^3. The large Ge(1)–O bond length is the one

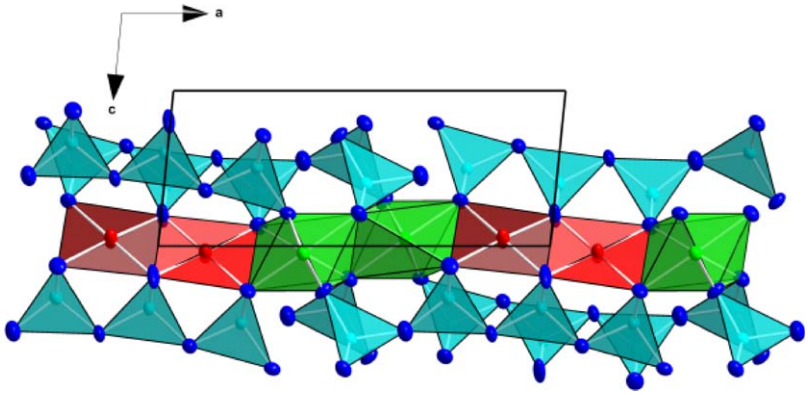

Fig. 3. Detail of the $Cu_2Sc_2Ge_4O_{13}$ structure showing the layers of Ge_4O_{13} chain segment in a view normal to (010).

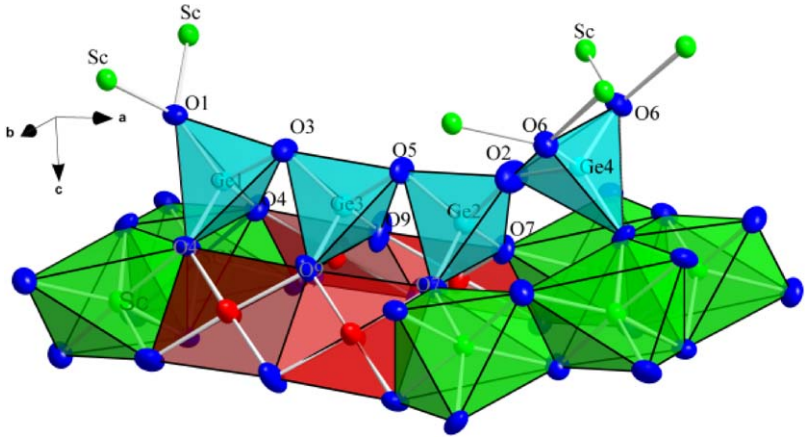

Fig. 4. Polyhedral representation of a Ge_4O_{13} chain segment and its interconnections with the ScO_6 octahedra and the CuO_4 plane.

to the O3 oxygen atom, common to the Ge(1)- and Ge(3)-tetrahedra. While the bond length distortion is low [BLD = 0.60(5)%] the tetrahedral angle variance is quite large [TAV = 24.5(2)°]. One corner (O(3) oxygen atom) of the $Ge(1)O_4$ tetrahedron is shared with the $Ge(3)O_4$ tetrahedron, one corner (O(1) oxygen atoms) is shared with two ScO_6 octahedra and the remaining two corners (O(4) oxygen atoms) are shared with one ScO_6 octahedron and a CuO_4 plane (Fig. 4). The $Ge(3)O_4$ tetrahedron is somewhat smaller and less distorted than the $Ge(1)O_4$ tetrahedron. Its mean Ge–O bond length amounts to 1.743(3) Å, which is the smallest of the four, and the tetrahedral volume is 2.72(1) $Å^3$. The bond length distortion is similar to the $Ge(1)O_4$ tetrahedron [BLD = 0.59(5)%], the quadratic variance of the bond angles, however is only 0.3(2)°, thus the oxygen coordination around the Ge(3) site is nearly perfect and this tetrahedron can be regarded as the most regular one out of the four. The $Ge(3)O_4$ tetrahedron is the one, which shares no common edge with ScO_6 octahedra. It shares two of its corners (O(3) and O(5) oxygen atoms) with the two neighboring GeO_4 tetrahedra, the two other corners are common to the tetrahedron and two CuO_4 planes via to O(9) oxygen atom, which exhibits rather pronounced anisotropic displacement parameters. The oxygen coordination around the Ge(2) site is somewhat more distorted that around Ge(3). This is expressed by the higher bond length distortion [BLD = 0.93(5)%] and the higher bond angle variance with TAV = 11.8(2)°. The $Ge(2)O_4$ tetrahedron shares two of its corners with neighboring tetrahedra (O(5) and O(2) oxygen atoms), the two other corners are common to the ScO_6 octahedron and the CuO_4 plane. The $Ge(4)O_4$ tetrahedron exhibits the smallest polyhedral volume [2.68(1) Å]. The bond length distortion is small; however, the tetrahedral angle variance is the largest (TAV = 36.9(2)°) among the four tetrahedral sites as is the tetrahedral quadratic elongation TQE [14]. Thus the $Ge(4)O_4$ tetrahedron can be regarded as the most distorted one. The $Ge(4)O_4$ tetrahedron is the one having the largest number of neighboring ScO_6 octahedra. One of the tetrahedral corners is shared with the $Ge(2)O_4$ tetrahedron; all other three corners are common to the tetrahedron and two ScO_6 octahedra (Fig. 4).

At 298 K several atoms show anisotropic atomic displacement parameters (ADP), among them Cu^{2+} with an ADP max/min axial ratio of the ellipsoid 3.5,

the O(2) oxygen atom and the O(5) oxygen atom (ADP max/min of 4.8 and 4.7, respectively) which are bridging oxygen atoms within the Ge_4O_{13} chain. The largest anisotropic thermal motion however is shown by the O(9) oxygen atom (ADP max/min = 6.4), which is common to two CuO_4 planes and the $Ge(3)O_4$ tetrahedron. The Ge atoms as well as Sc appear to be quite isotropic with ADP max/min ratios of 1.4–2.0. Oxygen atoms, which lie within the coordination sphere of Sc^{3+}, i.e. which are involved with the crankshaft-like chain of ScO_6 octahedra are distinctly less anisotropic with respect to their thermal motion. They are bonded much more rigidly, thus cannot vibrate as free as the other ones [O(2), O(5), O(9)]. Cooling to 100 K decreases the anisotropic displacement parameters by 30–40% on the average. In general, all atoms become less anisotropic. The ADP max/min ratio for the O(2) oxygen decreases to 2.8, the one of the O(5) oxygen atom to 1.9. However, the O(9) oxygen atom still shows a very anisotropic thermal motion with an ADP max/min ratio of 5.7 at 100 K (as compared to 6.4 at 298 K).

3.2. Comparison with other Cu-germanate compounds

In the following, we will compare—in brief—the title compound with some other Cu-germanates, reported in the literature [18–22]. $Cu_2M_2Ge_4O_{13}$ (M = Sc, Fe) shows some similarities with the crystal structure of the spin Peierl's compound $CuGeO_3$ (space group *Pbmm*). When the lengths of the germanate oligomer is increased, the infinite chain of $CuGeO_3$ is approached. Masuda et al. [2] thus proposed a hypothetical homologous series $(Cu^{2+}_{n-2}Fe^{3+}_2Ge_nO_{3n+1}$ with $n = 3, 4, \ldots, \infty)$. Having $n = 4$ corresponds to the structure of $Cu_2Sc_2Ge_4O_{13}$, studied here, if $n = \infty$ the hypothetical structure approaches the one of $CuGeO_3$ (Fig. 5). The b and c lattice parameters of the title compound (8.7034(9) and 4.8883(8) Å, respectively) are comparable to the corresponding lattice parameters in $CuGeO_3$ with $b = 8.4464(8)$ Å and $a = 4.7997(7)$ Å, respectively [18]. The c direction (a in $CuGeO_3$) is the one in which the layers of GeO_4 tetrahedral chains (oligomers) alternate with the layer of CuO_4 plaquettes.

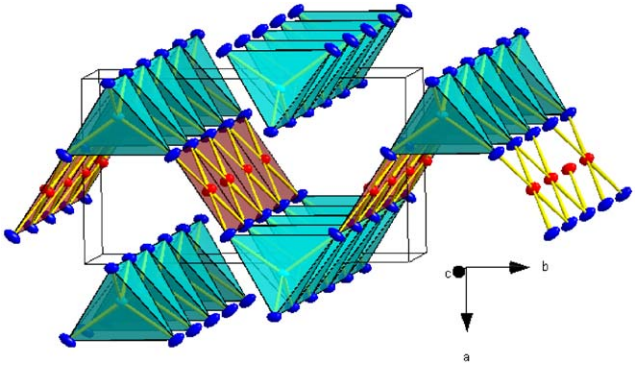

Fig. 5. Projections of the crystal structure of $CuGeO_3$ (data from Ref. [18]).

The coordination geometry of Cu is regular in $CuGeO_3$ having four identical Cu–O bond lengths of 1.934(1) Å [18] (thus a BLD of 0.0%) whereas it is distorted in the title compound. The shared O–O edge in $CuGeO_3$, connecting individual CuO_4 plaquettes to infinite chains, is 2.511(1) Å long, the unshared O–O edge one 2.943(1) Å, as compared to 2.456(4) Å and 3.006(4) and 3.028(4) in $Cu_2Sc_2Ge_4O_{13}$. Thus the ScO_6 chain not only cuts the CuO_4 chains into dimers, but also brings significant distortion to the CuO_4 unit and stretches it along a. What is identical in both structure types is the roof like arrangement of the CuO_4 units along the a-axis in $Cu_2Sc_2Ge_4O_{13}$ (Fig. 4) and along the c-axis in $CuGeO_3$ (Fig. 5). In contrast to the title compound with four symmetry independent Ge-positions, there is only one in $CuGeO_3$. By sharing a common corner, individual GeO_4 tetrahedra form an infinite straight chain running along c direction (the O–O–O bridging angle = 180°). Bringing the ScO_6 chain into the structure destroys these infinite straight chains thereby forming the bent Ge_4O_{13} tetramers of $Cu_2Sc_2Ge_4O_{13}$. In the light of distortional parameters, the GeO_4 tetrahedron in $CuGeO_3$ ($\langle$Ge–O$\rangle$ = 1.755(1) Å, BLD = 1.13%, TAV = 1.5° data calculated from Ref. [18]) best can be compared with the Ge(3) site in $Cu_2Sc_2Ge_4O_{13}$, which is the one having no common building units with the ScO_6 chain.

$Cu^{2+}R^{3+}_2Ge_4O_{12}$, R^{3+} = Ho, Er [19] also are similar to the title compound. These materials have P-1 symmetry and their structure was described by Cascales et al. [19] as being formed by "chains of RO_7 polyhedra, running in a direction, layers parallel to the ab plane containing $(GeO_4)_4$ tetrameric units and isolated CuO_6 distorted octahedra, which connect these units in the c direction as well as the RO_7 chains along b" [19]. The coordination polyhedra of the M sites (R^{3+}, Cu^{2+}) form layers within the ab plane, which alternate with layers of $(GeO_4)_4$ units along the c-direction. The c-lattice parameters of the $CuR_2Ge_4O_{12}$ compounds (4.89498(8) and 4.9075(1) Å for R = Ho and Er, respectively) are again similar to the one of the title compound. Within the proposed Cu-octahedra in $CuR_2Ge_4O_{12}$ the two long Cu–O distances are 2.779(4) and 2.794(4) Å (Ho and Er compound, respectively) away from the central Cu atom, so the coordination of the Cu^{2+}-atom may very well be described as being in a 4-fold planar coordination. Excluding these long Cu–O distances, the average Cu–O distances are 1.947(3) Å (Ho) and 1.954(3) Å (Er), close to the value of the title compound. As in $Cu_2Sc_2Ge_4O_{13}$ the CuO_4 units are distinctly elongated with O–O edge, shared with the RO_7 unit, being 2.630(7) and 2.871(8) Å long, the unshared O–O edge is 2.871(7) and 2.865(8) Å for R = Ho and Er, respectively. Within the ab plane, single RO_7 zig-zag

chains are connected to each other perpendicular to the chain direction by the CuO_4 units. The same connection mode is valid for the title compound, except the fact that Cu-dimers are formed here. Major differences between the two structure types are observed for the $(GeO_4)_4$ tetramers. Whereas in the title compound, the four symmetrically independent Ge^{4+} sites form linear, slightly bent units perpendicular to the ScO_6 chains, in $CuR_2Ge_4O_{12}$ the two symmetrically independent Ge^{4+} sites are arranged in an eclipsed configuration all sharing common corners with each other to form the $(GeO_4)_4$ unit. The GeO_4 tetrahedra in $CuR_2Ge_4O_{12}$ are distinctly more distorted than in $CuGeO_3$. In both compounds the Ge(1) site exhibit BLD of 1.5% and 1.3% and a very large TAV of 71.8° and 77.8° for R = Er and Ho, respectively (calculated from Ref. [19]). The Ge(2) site is more regular and exhibits polyhedra distortions comparable with the Ge(1) and Ge(2) sites in $Cu_2Sc_2Ge_4O_{13}$. The Ge(1) site in $CuR_2Ge_4O_{12}$ shares one of its edges with the RO_7 chain, whereas the Ge(2) site only shares common corners with it. As found for the title compound, the observation of an increasing tetrahedral distortion with an increasing amount of common building units between tetrahedral sites and the M-chain also holds true for the $CuR_2Ge_2O_{12}$. Another Cu-germanate compound being isotypic to $CuR_2Ge_4O_{12}$ (R = Er, Ho) is $CuYb_2Ge_4O_{12}$ [20].

As noted by Campá et al. [20] the crystal structure of $CuNd_2Ge_2O_8$, a Cu-germanate having *Cm* symmetry [21] is quite different from $CuR_2Ge_4O_{12}$ and thus from the title compound. $CuNd_2Ge_2O_8$ contains chains of much distorted CuO_6 octahedra (instead of isolated CuO_4 plaquettes), two different types of Ge-sites (GeO_4 tetrahedra and GeO_5 trigonal bipyramids) and rare earth $(RO_8)_4$ tetrameric units, which are connected to each other via two common corners. There is no structure in which layers of metal polyhedra alternate with layers of GeO_4 polyhedra like in all other Cu-germanate compounds discussed so far. A detailed comparison between $CuNd_2Ge_2O_8$ and $CuR_2Ge_4O_{12}$ is given by Campá et al. [20].

Contrarily to the above, the germanate $GdMnGe_2O_7$ [22] was found to show some topological similarities to $Cu_2Sc_2Ge_4O_{13}$. The compound has orthorhombic symmetry, space group $A222$, and shows a layered structure of metal sheets alternating with sheets of GeO_4 tetrahedral layers. The stacking is along the a-direction, the a unit cell parameter is 4.735(1) Å. It is close to the values found in the title compound, $CuGeO_3$ and $CuR_2Ge_4O_{12}$. $GdMnGe_2O_7$ is build up by chains of edge-sharing GdO_8 antiprisms which alternate with parallel chains of MnO_6 octahedra forming layers within the ab plane and linked together by Ge_2O_7 groups. If only the basal Mn^{2+}–O bond lengths are taken into account, which lie within 1.882(8)–1.933(11) Å [22], and excluding the two longer ones (2.463(3) Å), the GdO_8 chains are interconnected perpendicular to the chain direction via MnO_4 plaquettes (Fig. 6). This equatorial plane of the strongly elongated MnO_6 octahedron is stretched perpendicular to the chain direction with the shared O–O edge being 2.525(13) Å long, the unshared edge being 2.804(15) Å [22]. These values are of the same order of magnitude as those of the Cu-germanate compounds. The Ge_2O_7 groups are aligned parallel to the c-axis and slightly bent (O–O–O angle 169.7(1)°, Fig. 6). The GeO_4 tetrahedra are distinctly distorted and exhibit large bond lengths distortion (BLD = 2.0%) and a large tetrahedral angle variance (TAV = 76.4°).

3.3. Temperature dependent structural changes of $Cu_2Sc_2Ge_4O_{13}$ (100–298 K)

Except a, all lattice parameters decrease with decreasing temperature (Fig. 7). From a plot of the changes in lattice parameters relative to their values at 298 K (Fig. 7F) it is evident that the smallest change is observed for the monoclinic angle, the largest for the b-lattice parameter. The linear thermal expansion

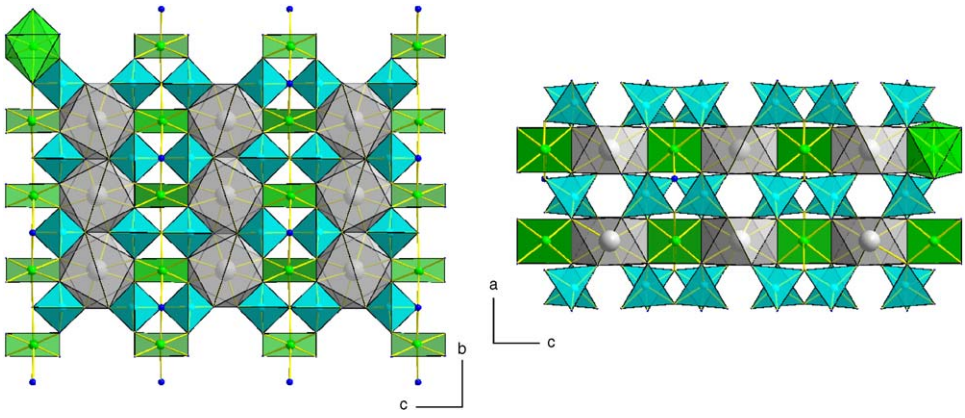

Fig. 6. Views of the structure of $GdMnGe_2O_7$ [22]. In the upper left Mn^{2+} is shown to be coordinated octahedrally, whereas for all other Mn^{2+} sites, only the equatorial plane of the octahedron is depict.

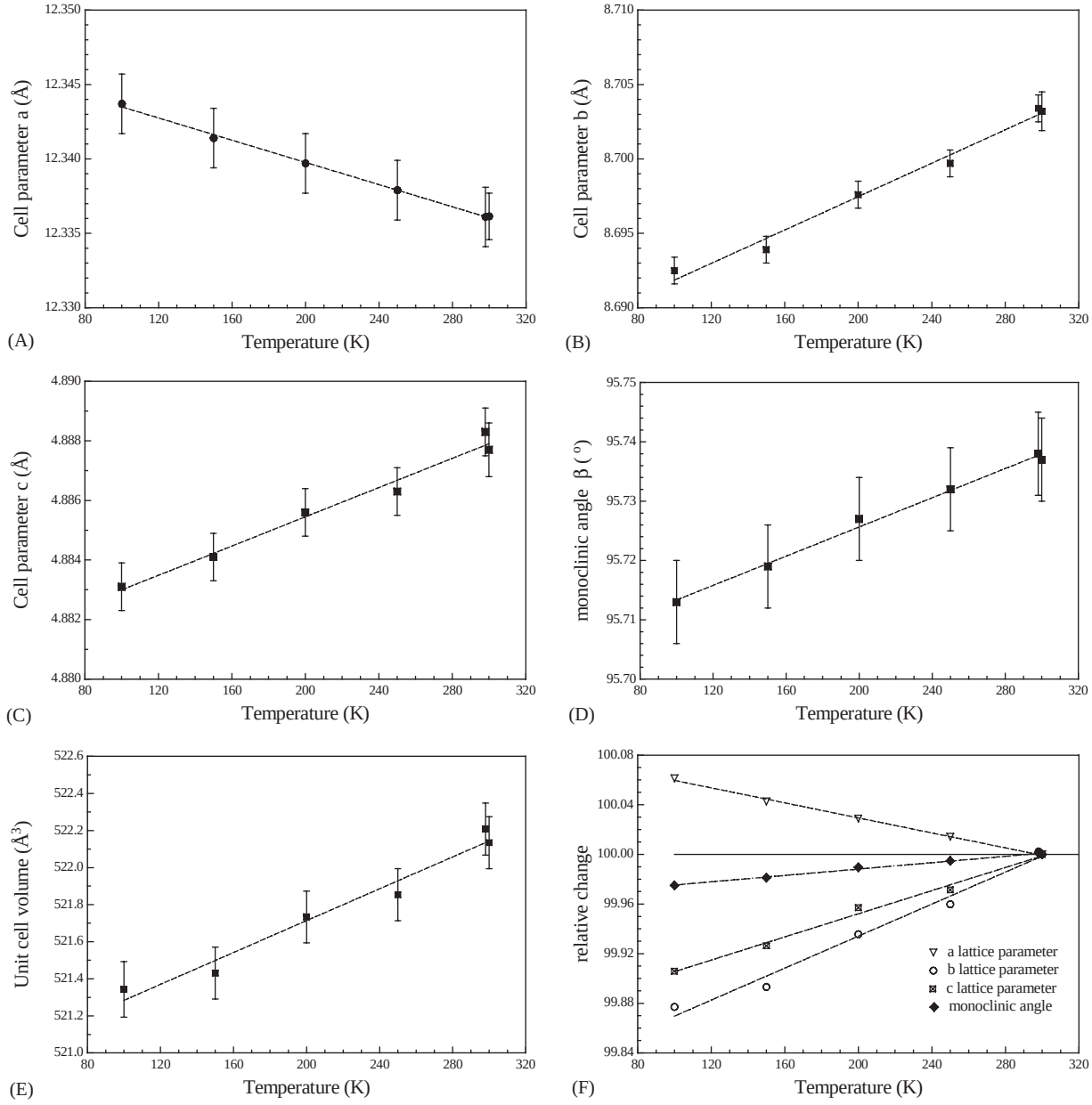

Fig. 7. Unit cell parameters of $Sc_2Cu_2Ge_4O_{13}$ as a function of temperature (A–E). In (F), the change of unit cell parameters relative to the value at 298 K is shown.

coefficients α were calculated to take values of $\alpha = -3.0(2) \times 10^{-6}$, $6.4(2) \times 10^{-6}$ and $5.0(2) \times 10^{-6}\,K^{-1}$ for the a, b and c lattice parameter, respectively, the volume expansion takes a value of $\alpha = 8.3(2) \times 10^{-6}\,K^{-1}$. Thereby α is given by: $\alpha = (a_T - a_0)/(a_0(T - T_0)$ with a_0 = lattice parameter at the reference temperature T_0 (100 K in our case) and a_T = lattice parameter at the temperature T.

On the average, the Sc–O bond length remains constant within experimental error when temperature is lowered. However, some of the individual Sc–O bond lengths significantly decrease in size with decreasing temperature (as would be expected), some of them increase (Table 4). These alterations cause the bond length distortion to decrease as temperature drops, whereas the octahedral angle variance increases with decreasing temperature from 208.9(2)° to 212.2(2)°. Thus the octahedra appear to be more distorted at low temperature. This behavior also is supported by an increase of the edge length distortion ELD (Table 4) at low temperatures. For the O–O octahedral edges the distinct increase of the smaller O(6)–O(7) octahedral edge—pointing in a-direction—and the longer O(6)–O(7) edge increase distinctly with decreasing temperature (Table 4). This behavior correlates well with the increasing a-lattice parameter, when temperature

Table 4
Selected bond lengths, bond angles, interatomic distances and distortion parameters for $Cu_2Sc_2Ge_4O_{13}$ at different temperatures

	100 K	150 K	200	250 K	298 K
Sc–O6 (Å)	2.064(3)	2.061(3)	2.059(3)	2.059(3)	2.057(4)
Sc–O7 (Å)	2.091(4)	2.088(3)	2.088(3)	2.083(3)	2.081(3)
Sc–O8 (Å)	2.117(3)	2.118(3)	2.118(3)	2.119(3)	2.119(3)
Sc–O1 (Å)	2.119(3)	2.120(3)	2.123(3)	2.124(3)	2.126(3)
Sc–O4 (Å)	2.121(3)	2.122(3)	2.123(3)	2.128(3)	2.128(3)
Sc–O6 (Å)	2.162(3)	2.158(4)	2.157(3)	2.163(3)	2.162(4)
⟨Sc–O⟩ (Å)	2.112(3)	2.111(3)	2.111(3)	2.112(3)	2.112(3)
BLD (%)	1.10(5)	1.15(5)	1.21(5)	1.30(5)	1.37(5)
ELD (%)	9.70(5)	9.69(5)	9.67(5)	9.65(5)	9.60(5)
OAV (deg)	210.2(2)	211.3(2)	211.3(2)	209.0(2)	209.9(2)
Volume (Å^3)	11.566(7)	11.516(7)	11.537(6)	11.565(7)	11.566(7)
Cu–O9 (Å)	1.938(2)	1.938(3)	1.934(3)	1.931(3)	1.931(4)
Cu–O4 (Å)	1.945(3)	1.945(3)	1.947(3)	1.945(3)	1.947(3)
Cu–O9 (Å)	1.955(2)	1.956(4)	1.955(3)	1.954(4)	1.945(4)
Cu–O9 (Å)	1.995(4)	2.004(4)	2.002(3)	2.009(2)	2.011(4)
⟨Cu–O⟩ (Å)	1.958(3)	1.961(4)	1.960(3)	1.960(3)	1.961(4)
BLD (%)	0.93(5)	1.09(5)	1.08(5)	1.24(5)	1.28(5)
Cu–Cu (Å)	3.024(1)	3.021(1)	3.015(1)	3.023(1)	3.011(1)
Cu–Sc (Å)	3.127(1)	3.128(1)	3.130(1)	3.129(1)	3.129(1)
Sc–Sc (Å)	3.302(1)	3.303(1)	3.304(1)	3.304(1)	3.306(1)
Sc–Sc (Å)	3.397(1)	3.396(1)	3.397(1)	3.399(1)	3.400(1)
Cu–O9–Cu (deg)	101.95(12)	101.74(12)	101.62(12)	101.69(14)	101.60(13)
Sc–O6–Sc (deg)	106.98(11)	107.17(11)	107.23(12)	107.22(13)	107.35(13)
Sc–O1–Sc (deg)	102.42(14)	102.32(13)	102.25(13)	102.12(13)	101.95(14)
Ge1–O1 (Å)	1.741(5)	1.743(2)	1.737(3)	1.738(4)	1.734(5)
Ge1–O4 (Å)	1.746(4)	1.747(2)	1.744(3)	1.746(3)	1.750(4)
Ge1–O3 × 2 (Å)	1.771(2)	1.772(4)	1.772(4)	1.772(4)	1.773(5)
⟨Ge1–O⟩ (Å)	1.751(3)	1.752(3)	1.749(3)	1.750(4)	1.751(4)
BLD (%)	0.57(5)	0.56(5)	0.65(5)	0.62(5)	0.60(5)
TAV (deg)	25.5(2)	25.1(2)	26.7(2)	24.9(2)	24.5(2)
Volume (Å^3)	2.729(8)	2.733(7)	2.721(8)	2.726(7)	2.732(7)
Ge2–O2 (Å)	1.720(5)	1.712(2)	1.709(4)	1.707(5)	1.707(5)
Ge2–O7 × 2(Å)	1.744(4)	1.741(3)	1.744(4)	1.743(4)	1.742(3)
Ge2–O5 (Å)	1.769(4)	1.771(4)	1.774(5)	1.766(5)	1.769(5)
⟨Ge2–O⟩ (Å)	1.744(4)	1.741(3)	1.743(4)	1.739(5)	1.739(4)
BLD (%)	0.70(5)	0.85(5)	0.96(5)	0.95(5)	0.93(5)
TAV (deg)	12.7(2)	12.2(2)	13.3(2)	13.3(2)	11.8(2)
Volume (Å^3)	2.7107(8)	2.696(7)	2.703(8)	2.687(7)	2.688(7)
Ge3–O9 × 2 (Å)	1.734(3)	1.734(3)	1.733(3)	1.734(3)	1.733(4)
Ge3–O3 (Å)	1.744(2)	1.742(5)	1.744(3)	1.745(5)	1.743(4)
Ge3–O5 (Å)	1.757(5)	1.758(2)	1.759(4)	1.761(5)	1.764(5)
⟨Ge3–O⟩ (Å)	1.742(4)	1.74(4)	1.742(3)	1.744(4)	1.743(4)
BLD (%)	0.47(5)	0.47(5)	0.53(5)	0.53(5)	0.59(5)
TAV (deg)	0.3(2)	0.5(2)	0.3(2)	0.4(2)	0.3(2)
Volume (Å^3)	2.714(8)	2.711(8)	2.715(8)	2.720(8)	2.719(8)
Ge4–O2 (Å)	1.734(5)	1.739(3)	1.743(3)	1.747(3)	1.738(5)
Ge4–O8 (Å)	1.742(5)	1.742(5)	1.744(3)	1.743(3)	1.735(5)
Ge4–O6 × 2 (Å)	1.743(4)	1.744(3)	1.749(3)	1.747(3)	1.750(4)
⟨Ge4–O⟩ (Å)	1.741(4)	1.742(3)	1.746(3)	1.746(3)	1.743(5)
BLD (%)	0.19(5)	0.10(5)	0.16(5)	0.07(5)	0.40(5)
TAV (deg)	38.1(2)	36.9(2)	37.1(2)	38.8(2)	36.9(2)
Volume (Å^3)	2.664(7)	2.674(8)	2.691(8)	2.688(8)	2.678(8)

$\mathrm{BLD} = \frac{100}{n}\sum_{i=1}^{n}\frac{|(X-\mathrm{O})_i - (\langle X-\mathrm{O}\rangle)|}{(\langle X-\mathrm{O}\rangle)}\%$, n = amount of cation–anion bonds and X–O = cation–anion (oxygen) distance [14]; $\mathrm{ELD} = \frac{100}{n}\sum_{i=1}^{n}\frac{|(\mathrm{O}-\mathrm{O})_i - (\langle \mathrm{O}-\mathrm{O}\rangle)|}{(\langle \mathrm{O}-\mathrm{O}\rangle)}\%$, n = amount of edges and (O–O) = oxygen–oxygen interatomic distance defining an edge of the octahedron [14]; $\mathrm{OAV} = \sum_{i=1}^{12}(\Theta_i - 90^\circ)^2/11$ with Θ_i = O–M–O bonding angle [15]; $\mathrm{TAV} = \sum_{i=1}^{6}(\Theta_i - 109.57^\circ)^2/5$ with Θ_i = O–T–O bonding angle [15].

decreases. The Sc^{3+}–Sc^{3+} interatomic distance, which is along the crystallographic *b*-direction and which intersects the O(1)–O(8) common edge between two neighboring ScO_6 octahedra, decreases with decreasing temperature. This correlates well with the decrease of the Sc–O(1) bond lengths. Thereby the Sc–O(1)–Sc bond angle increases slightly from 101.95(8)° at 298 K to 102.32(9)° at 100 K and compensates partly for the distinct decrease of the Sc–O(1) bond lengths. The longer Sc^{3+}–Sc^{3+} as well as the Sc^{3+}–Cu^{2+} interatomic distances, which both points towards the *a*-direction remain constant within experimental error between 100 and 298 K.

Within the Cu^{2+} coordination the most pronounced change is observed for the Cu–O(7) bond, which contracts significantly by ≈0.017(4) Å. The O(7) oxygen atom is common to the CuO_4 plane and the ScO_6 octahedron. The Cu–O(4), as well as the longer Cu–O(9) bond stay constant, whereas the shorter Cu–O(9) bond increases with decreasing temperature (Fig. 8A). The most evident and important change concerns the Cu–Cu interatomic distance, which increases significantly with decreasing temperature. It is assumed that this is the main reason for the negative thermal expansion of the *a* lattice parameter (Fig. 8B). The increase of the Cu–Cu interatomic distance is partly brought about by the increase of the shorter Cu–O(9) bond length but mainly by an increase of the Cu–O(9)–Cu bond angle, which increases from 101.50(8)° at 298 K to 101.95(9)° at 100 K.

The GeO_4 tetrahedra are rigid units, which show only small temperature variations. The bonds, which show a temperature variation, are associated with the oxygen atoms, bridging the tetrahedra along the axis O(1)–O(3)–O(5)–O(2). For all GeO_4 tetrahedra, the bond length distortion BLD decreases with decreasing temperature, whereas the tetrahedral angle variance remains constant (Ge(2)-site) or increases. The bridging angle O(1)–O(3)–O(5) remains constant, the O(3)–O(5)–O(2) angle shows a tendency to decrease with decreasing temperature by about 0.5°. However, only the O(5)–O(2)–O(6) angle shows a smooth temperature variation and increases with decreasing temperature by 0.75°. So there are only minor changes within the bending mode of the Ge_4O_{13} tetramer, which may be associated with the increase of the Cu–Cu interatomic distance with decreasing temperature.

4. Conclusion

- The structure of $Cu_2Sc_2Ge_4O_{13}$ is isotypic to the one recently described in Refs. [1,2] for $Cu_2Fe_2Ge_4O_{13}$. The quantitative differences between the two compounds are due to the substitution of the smaller Fe^{3+} (ionic radius $I_R = 0.645$ Å [11]) by the larger Sc^{3+} ion ($I_R = 0.72$ Å [11]).
- The above mentioned substitution results in an expansion of the unit cell in the *a* and *b* direction, whereas the *c* direction is not affected. The expansion of the octahedral chain in *c* is compensated by larger O1–O3–O5 and O3–O5–O2 bridging angles within the Ge_4O_{13} chain in $Cu_2Sc_2Ge_4O_{13}$, as compared to $Cu_2Fe_2Ge_4O_{13}$ (171.7(1)° and 171.8(1)°, respectively). When viewed along [010], the Ge_4O_{13} chain segment is less bent in the title compound and thus reduces the thickness requirement of the tetrahedral sheet in *c*.
- The average Sc–O bond length is—of course—larger than the average Fe–O length. The difference in mean bond length is very similar to the difference in the ionic radii of the two cations. The $Sc^{3+}O_6$ octahedron reveals polyhedral distortion parameters similar to the $Fe^{3+}O_6$ octahedron. While the bond length distortion is similar, the octahedral angle variance as well as the edge length distortion is larger in the Sc^{3+} compound. All in all, the oxygen coordination around the Sc^{3+} site is very far from the one of an ideal octahedron.
- The most regular tetrahedral oxygen coordination is the one around the Ge(3) site. This $Ge(3)O_4$

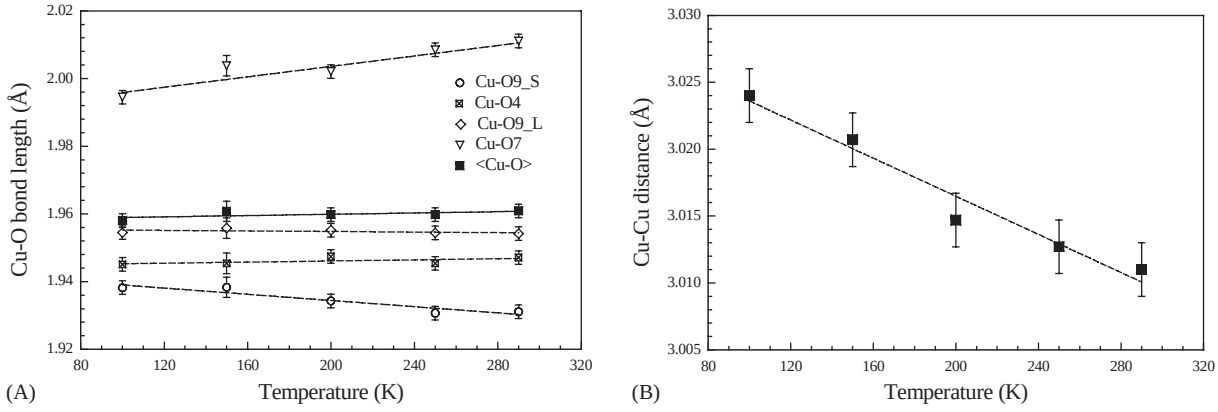

Fig. 8. Cu–O bond lengths for $Sc_2Cu_2Ge_4O_{13}$ as a function of temperature (A) and Cu–Cu interatomic distance for $Sc_2Cu_2Ge_4O_{13}$ as a function of temperature (B).

coordination polyhedron shares no common corner with a ScO_6 octahedron. The most distorted tetrahedral oxygen coordination can be found for the Ge(4) site. It is the site with the highest number of neighboring ScO_6 octahedra. Compared to the $Cu_2Fe_2Ge_4O_{13}$ compound [1,2] the average Ge–O bond lengths are generally shorter by 0.004–0.010 Å in the title compound. The bond length distortions [11] are larger but still small in $Cu_2Sc_2Ge_4O_{13}$ and the tetrahedral angle variance TAV [13] is distinctly smaller as compared to $Cu_2Fe_2Ge_4O_{13}$ (38.8(2)°, 27.0(2)°, 1.5(2)° and 59.7(2)° for the Ge(1), Ge(2), Ge(3) and Ge(4) site, respectively [1]). Thus, it can be concluded, that the GeO_4 tetrahedra are more regular in the title compound. However, in the Fe analogue, the Ge(3) site also reflects nearly perfect tetrahedral geometry, whereas the Ge(4) site is the most distorted one.

- Decreasing temperature to 100 K does not change the crystallographic symmetry of the title compound.
- Upon cooling, all unit cell parameters decrease except the *a*-lattice parameter, which shows a negative thermal expansion. This correlates very well with the increase of the Cu^{2+}–Cu^{2+} interatomic distance (which is aligned parallel to the *a* axis) when temperature decreases. The Cu^{2+}–Sc^{3+} as well as the Sc^{3+}–Sc^{3+} interatomic distances, which run along the *a*-axis, remain constant or decrease with decreasing temperature.
- Both, the average Cu^{2+}–O and the average Sc^{3+}–O bond length remain constant. However, some distinct temperature dependent alterations of individual bond lengths take place upon cooling, especially within the octahedral site.

Acknowledgments

GJR thank the Austrian Academy of Science (APART, Austrian Program of Advanced Research and Technology) and the Austrian "Fond zur Förderung der Wissenschaftlichen Forschung", FWF (grant R33-N10) for financing the research activities. We also thank the anonymous reviewers who help to increase the impact of the paper with their constructive comments.

References

[1] G.J. Redhammer, G. Roth, Z. Kristallogr. 20 ((Suppl.) (2003) 148.
[2] T. Masuda, B.C. Chakoumakos, C.L. Nygren, S. Imai, K.J. Uchinokura, J. Solid State Chem. 176 (2003) 175.
[3] H. Völlenke, A. Wittmann, H. Nortny, Monatsh. Chem. 98 (1967) 1352.
[4] M. Hase, K. Terasaki, K. Uchinokura, Phys. Rev. Lett. 70 (1993) 3651.
[5] G.J. Redhammer, W. Treutmann, M. Merz, G. Tippelt, G. Roth, W. Lottermoser, E. Dachs, G. Amthauer, Acta Crystallogr. B, submitted for publication.
[6] Stoe & Cie, X-SHAPE and X-RED: Programs for Optimisation of the Crystal SHAPE (w.r.t the Merging *R*-value) and Numerical Absorption Correction, Stoe & Cie, Darmstadt, Germany, 1996.
[7] G.M. Sheldrick, SHELXS-97 and SHELXS-97: Programs for Crystal Structure Solution and Refinement, University of Göttingen, Germany, 1997.
[8] L.J. Farrugia, J. Appl. Crystallogr. 32 (1999) 837.
[9] A.J.C. Wilson (Ed.), International Tables for Crystallography, Vol. C, Kluwer Academic Publishers, Dordrecht, The Netherlands, 1992.
[10] K. Brandenburg, M.J. Berndt, Appl. Crystallogr. 32 (1999) 1028.
[11] A.S. Wills, I.A. Brown, VaList: Bond Valence Calculation Program V.1.0, CEA, France, 1999.
[12] N.E. Brese, M. O'Keeffe, Acta Crystallogr. B 47 (1991) 192.
[13] R.D. Shannon, C.T. Prewitt, Acta Crystallogr. B 25 (1969) 925.
[14] B. Renner, G. Lehmann, Z. Kristallogr. 175 (1986) 43.
[15] K. Robinson, G.V. Gibbs, P.H. Ribbe, Science 172 (1971) 567.
[16] G.J. Redhammer, G. Roth, Z. Kristallogr. 217 (2002) 63.
[17] G.J. Redhammer, G. Roth, Am. Mineral. 87 (2002) 1464.
[18] M. Braden, E. Ressouche, B. Büchner, R. Kessler, G. Heger, G. Dhalenne, A. Revcolevschi, Phsy. Rev. B 57 (1998) 57.
[19] C. Cascales, M.T. Fernandez Diaz, M.A. Monge, Chem. Mater. 12 (2000) 3369.
[20] J.A. Campá, C. Cascales, E. Gutiérrez-Puebla, M.A. Monge, I. Rasines, C. Ruíz Valero, J. Solid State Chem. 124 (1996) 17.
[21] J.A. Campá, E. Gutiérrez-Puebla, M.A. Monge, C. Ruíz Valero, J. Mira, J. Rivas, C. Cascales, I. Rasines, J. Solid State Chem. 120 (1995) 254.
[22] C. Taviot-Guého, P. Léone, P. Palvadeau, J. Rouxel, J. Solid State Chem. 143 (1999) 145.